Available online at www.sciencedirect.com
ScienceDirect
Ceramics International 36 (2010) 2011–2016
CERAMICS INTERNATIONAL
www.elsevier.com/locate/ceramint

Testing media influences on the dielectric properties of lead sodium niobate glass-ceramics

D.F. Han, Q.M. Zhang, Q. Tang, J. Luo, J. Du *

Advanced Electronic Materials Institute, General Research Institute for Nonferrous Metals, Beijing 100088, China

Received 26 February 2010; received in revised form 12 March 2010; accepted 10 April 2010
Available online 20 June 2010

Abstract

The influences of testing media on the breakdown strength (BDS) and dielectric properties of glass-ceramics in the Na_2O–PbO–Nb_2O_5–SiO_2 system were investigated. This work was brought out by consideration of the electric conductance, dielectric constant and breakdown strength of different testing media, which are the main reasons for the different dielectric properties and BDS values of the identical dielectric sample. Leakage current (LC), *P–E* hysteresis loops, *C–V* curves and breakdown tests show that the BDS and the dielectric properties of the glass-ceramics could be optimized through using appropriate testing medium. It turns out that three favorable characteristics of the dielectric composites could be optimized in silicon/castor oil mixture: the lowest LC (LC = 6.72×10^{-6} A, at $E = 25$ kV/mm), thin *P–E* hysteresis loops and low hysteresis. Furthermore, the highest BDS of the glass-ceramic was obtained in glycerin (BDS = 105.6 kV/mm with sample thickness of 0.108 mm) compared to other media.

Keywords: C. Dielectric properties; D. Niobates; D. Glass-ceramics; Testing media

1. Introduction

Test condition plays a very important role in dielectric properties measurement. The measured results of some specific properties of dielectric materials, such as breakdown strength, leakage current and *P–E* hysteresis loops, are usually sensitive to the testing environment and also the electrode geometry. To date, the main focus of improvement has been on the influences of the electrodes [1–3]. However, the testing media, especially the testing liquids, also have major impacts on the measured results of the dielectric performance.

Liquid testing media have been widely used to prevent flashover and corona discharge in dielectric properties measurement at high voltage. Traditionally, silicon oil has been mainly used as the testing medium in breakdown strength (BDS) tests [4–7] and *P–E* hysteresis loops measurements [8]. In addition, some work was about the application of transformer oil [9]. Both of the above mentioned oils are low dielectric constant liquids. Also, these are some other work concerning the use of high dielectric constant liquid media. Luo et al. [3] performed dielectric failure measurement in ethylene glycol/water mixture, and observed high breakdown strength of dielectrics. However, it appears highly necessary to establish a detailed relationship between the liquid media characteristics and the measured dielectric properties, especially when it concerns about dielectric materials with high dielectric constant and high breakdown strength, such as in the case of glass-ceramics.

In the present paper, we investigated the relationship between different testing media and the measured properties of the dielectrics. A modeled glass-ceramic based on lead sodium niobates was used as the dielectric material to approach to the optimal value of its dielectric properties. The relationship between the measured BDS of the dielectric material and the dielectric constant of the liquid media has been discussed.

2. Experimental procedure

Lead sodium niobates based glass-ceramic dielectrics consisting of high BDS glass phase and high dielectric constant ceramic phases, $Pb_2Nb_2O_7$ and $NaNbO_3$ [3], were provided for the samples. The dielectric constant and dielectric loss of this

* Corresponding author. Tel.: +86 10 82241247.
E-mail address: dujun@grinm.com (J. Du).

0272-8842/$36.00
doi:10.1016/j.ceramint.2010.05.009

Table 1
Characteristics of some testing liquid media.

Medium	Dielectric constant	BDS (kV, 2.5 mm)	Leakage current (2 kV/1 cm)	Thermal conductivity (W/m K)
Silicon oil	2.2–2.6	13.7–17.7	8.56×10 PP^{-9} PPA/cmPP^2	0.1
Transformer oil	2.2	35–50	3.97×10 PP^{-9} PPA/cmPP^2	0.128
Silicon/castor oil	3.5–3.9	19.9–21.9	2.40×10 PP^{-9} PPA/cmPP^2	0.14
Glycerin	37	~20	3.45×10 PP^{-3} PPA/cmPP^2	0.276
Glycol	42.5	~20	4.23×10 PP^{-3} PPA/cmPP^2	0.252

glass-ceramic are 170 and 0.0098 at 1 kHz, respectively. Five different testing liquids were selected and studied in this work according to their typical characteristics, as summarized in Table 1. The glass-ceramics were cut and polished into sheets of 0.05–0.40 mm in thickness. Then, Au metal films, as contact electrodes of the plane dielectric capacitor, were coated on both surfaces of the glass-ceramic samples by DC magnetron sputtering (Model JK-200B, Instrument Company, Ltd., Beijing, China).

The morphology of glass-ceramic samples and perforation after breakdown test were observed by field-emission scanning electron microscopy (FE-SEM; Model S-4800, HITACHI, Japan). The breakdown strengths were measured by a Tektronix AFG 3021 Arbitrary/Function Generator (Beaverton, OR) and a Trek Model 30/20A high-voltage amplifier (Beaverton, OR) under 1 Hz AC triangle wave with a rate of increase of 300 V/step in silicon oil (SO), silicon/castor oil mixture (SCO), transformer oil (TO), glycol (GO) and glycerin (GE), respectively. Furthermore, leakage currents, *P–E* hysteresis loops and capacitance–voltage (*C–V*) curves were measured using a ferroelectric tester (RT6000HVA, Radiant Technology, Albuquerque, NM).

3. Results and discussion

3.1. Dielectric properties

As shown in Fig. 2, prior to 20 kV/mm, there is no significant difference in leakage currents of the glass-ceramics tested in SO, TO and SCO, while $j_{LC}(\mathrm{SO}) > j_{LC}(\mathrm{TO}) > j_{LC}(\mathrm{SCO})$ is evidenced after 20 kV/mm. Also, the leakage current densities tested in glycol and glycerin are $\sim 10^{-3}$ A/cm^2, which are five orders of magnitude higher than those tested in the other three liquids. This is due to the high electric conductivity of GO and GE (10^{-3} A/cm^2, shown in Table 1). Thus, in what follows, only transformer oil (TO), silicon oil (SO) and silicon/castor oil mixture (SCO) testing liquids were used to study the leakage current density–electric field (*j–E*) behavior of the dielectric glass-ceramic samples in order to establish the relationship between the measured leakage current of the dielectric glass-ceramic and the electric conductivity of the liquid media.

In Fig. 3(a) are shown the current–voltage (*I–V*) results of the dielectric glass-ceramic measured in these three testing media. Obviously, the leakage current increased with the electric conductivity of the liquid media. The conduction mechanism of the dielectric glass-ceramic can be analyzed by three regions as seen in Fig. 3(a), i.e. Ohmic conductivity region, region of exponential current increase and region of vertical current enhancement. The resistivity values ($\approx 1 \times 10^{10}\ \Omega$ m) of the dielectrics with nano-sized ceramic phases embedded in glass matrix (as shown by the FE-SEM image in Fig. 1) via controlled crystallization process [10] were determined for Ohmic part. Since the $\ln j$ versus $E^{1/2}$ plot is the best liner fitted line which is shown in Fig. 3(b), the second part on the *I–V* curves might be governed by Schottky emission [11,12]. A similar phenomenon was also observed in (Ba,Sr)TiO_3 ferroelectric ceramics on copper by Dedyk et al. [13]. The third part of the vertical current increase may be related to the regime of the complete filling of deep traps [13,14]. The practically vertical *I–V* dependence could be interpreted as dielectric breakdown; however, the electrical properties of the sample were restored after a voltage decrease [13] (Figs. 2 and 3).

Due to the large leakage current, curves tested in glycol (GO) and glycerin (GE) cannot exhibit *P–E* hysteresis loops [15]. The *P–E* hysteresis loops tested in SO, TO and SCO are plotted in Fig. 4. Obviously, it can be seen that the *P–E* loops get thick accompanied by the increase of dielectric leakage current. Due to the largest electric conductivity of SO, the dielectric glass-ceramic shows the pronounced broadening *P–E* loops (indicating an increases in dielectric loss) [16], while the thin *P–E* hysteresis loops tested in SCO is possibly induced by the lowest leakage current of the SCO. In Fig. 5 are illustrated the DC bias voltage dependence of dielectric constant of the glass-ceramic tested in transformer oil (TO), silicon oil (SO) and silicon/castor oil mixture (SCO). The glass-ceramic

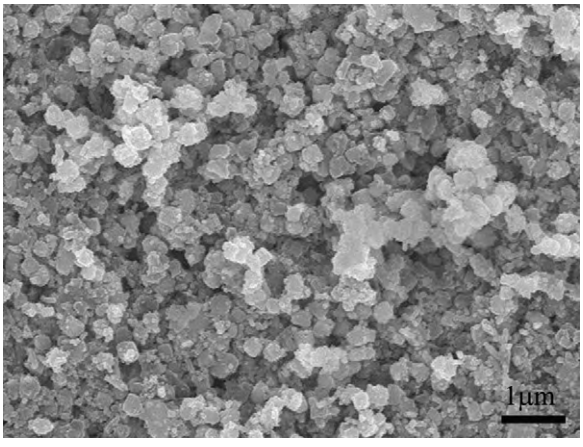

Fig. 1. FE-SEM micrograph of glass-ceramics.

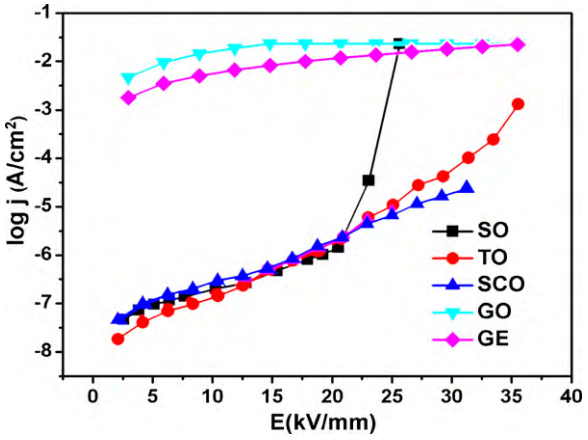

Fig. 2. Log(j) versus E plots of the dielectric in different testing media.

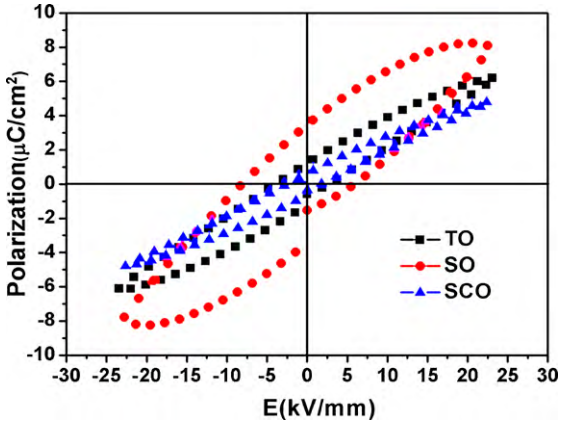

Fig. 4. P–E hysteresis curves for the dielectric tested in TO, SO and SCO.

showed comparatively low hysteresis on the capacitance–voltage (C–V) characteristics, which can lead to the linear P–E hysteresis loop. Since capacitance measurement depends on the charge of the electrode surface, and also, due to $j_{LC}(\mathrm{SO}) > j_{LC}(\mathrm{TO}) > j_{LC}(\mathrm{SCO})$, $\Delta\varepsilon_r/\varepsilon_r(\mathrm{SO}) > \Delta\varepsilon_r/\varepsilon_r(\mathrm{TO}) > \Delta\varepsilon_r/\varepsilon_r(\mathrm{SCO})$ as indicated in Fig. 5 leads to the minimum rate of the dielectric constant change in silicon/castor oil mixture.

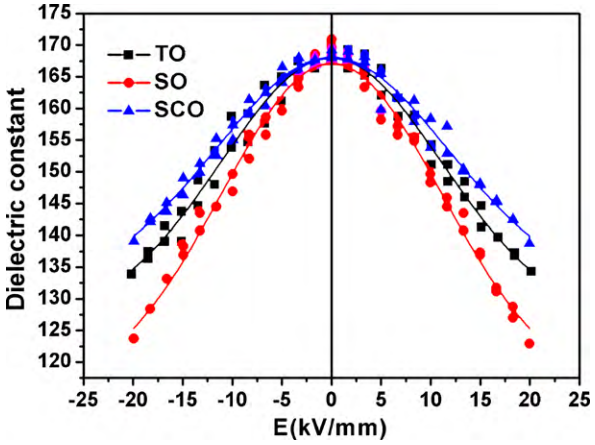

Fig. 5. DC bias voltage dependence of dielectric constant of the glass-ceramic in TO, SO and SCO.

3.2. Breakdown strength

Breakdown concerns dielectrics submitted to high field, which corresponds to the loss of insulating properties and mechanical degradation of the material [9]. Fig. 6 shows the perforation of a dielectric sheet (crater, channel, crack and melting local) caused by the flow of a breakdown current. The breakdown process is associated with an explosive, sparking event caused melting within the crater, where the crystallization structure formed varies with the host dielectric. For all the dielectrics there was a variation in the breakdown strength with sheet thickness, since, with specimen thickness increasing, there is an increasing probability of the presence of a breakdown initiating flaw [17]. Fig. 7 shows the breakdown strength results for lead sodium niobated glass-ceramics in different testing liquid media. It is clearly seen that the increase in breakdown strength not only depends on the thickness decreasing of the dielectrics, but also depends on the dielectric constant increasing of the testing media. The highest value of the dielectric strength was obtained in glycerin (BDS = 105.6 kV/mm at d = 0.108 mm).

In consideration of the fact that the breakdown is usually happens on the sample surface as illustrated in Fig. 8, the voltage distribution of the dielectric and the testing liquid media can be estimated by the two-layer dielectrics series model (TLDSM) analysis, which is shown in Fig. 9. Fig. 10

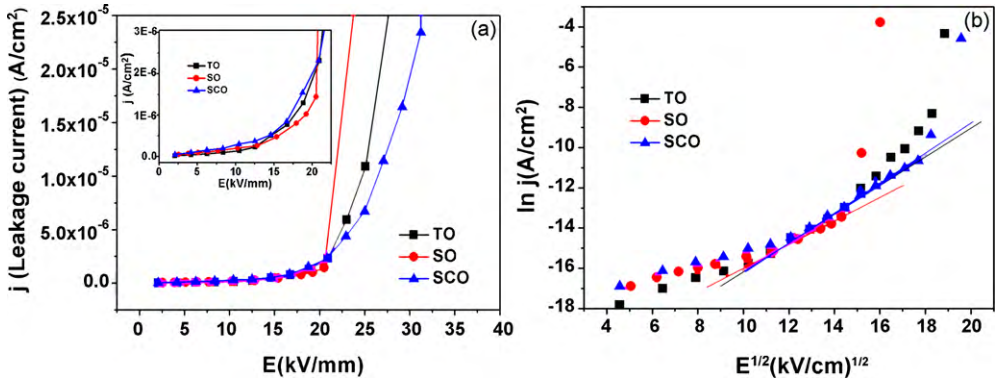

Fig. 3. Current–voltage (I–V) characteristics (a) and the ln j versus $E^{1/2}$ plot (b) (the solid lines are used to fit the experimental data) of the dielectric in transformer oil (TO), silicon oil (SO) and silicon/castor oil mixture (SCO).

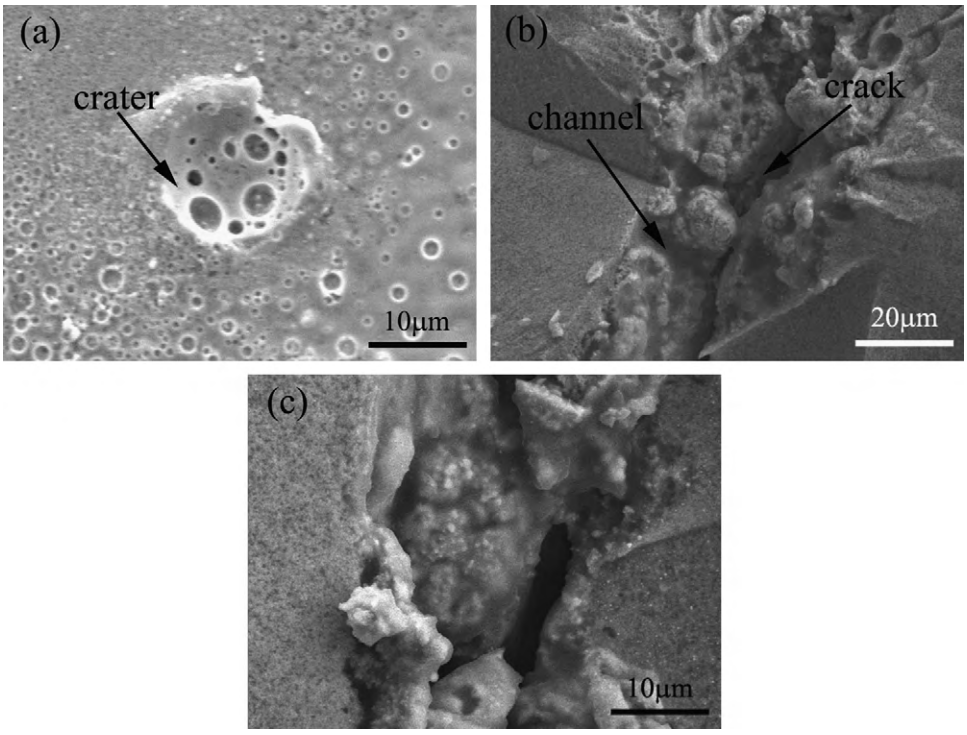

Fig. 6. Perforation of the glass-ceramic sample after breakdown test: SEM observation of (a) the crater appeared on the surface of the dielectric, (b) the channel and the crack crossing the insulator and (c) the local melting.

shows that the voltage waveform is a standard monopolar triangular one that can be simply defined by providing the maximum voltage and the entire duration of the waveform in nanoseconds (4 ns) which is much shorter than the polarization time ($\sim 10^{-6}$ s). Therefore, the two-layer dielectrics series model (TLDSM) is in the state of charge when the waveform begins at 0 V, steps to the maximum value of the assigned voltage and then proceeds to step to 0 V. To sum up, according to the above analysis, the dielectric strength distribution of the TLDSM can be analyzed by Gauss' Law for the dielectric, which is written as

$$\oiint_s \vec{D} d\vec{S} = \sum_i q_i, \quad \vec{D} = \varepsilon_r \varepsilon_0 \vec{E} \tag{1}$$

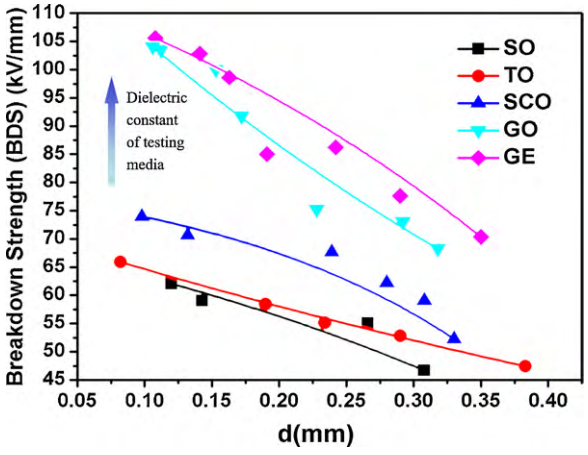

Fig. 7. Relationship between breakdown strength (BDS) and sheet thickness (d) in different testing media.

where $\vec{D}$ and $\vec{S}$ are the vector of the electric displacement and the Gauss face, respectively, while q_i is the free electric charge in the Gauss face, and ε_0 and ε_r are the permittivity of free space (8.854×10^{-12} Fm^{-1}) and relative permittivity, respectively. Since the free electric charge in the closed Gauss face $\vec{S}$ (the dotted line in the middle of the model) which is shown in Fig. 9(b) is zero, according to Gauss' law for the dielectric, the relation between D_{g-c} and D_m is given by

$$\oiint_s \vec{D} d\vec{S} = -D_{g-c}S + D_m S = 0$$

thus,

$$\frac{E_{g-c}}{E_m} = \frac{\varepsilon_m}{\varepsilon_{g-c}} \tag{2}$$

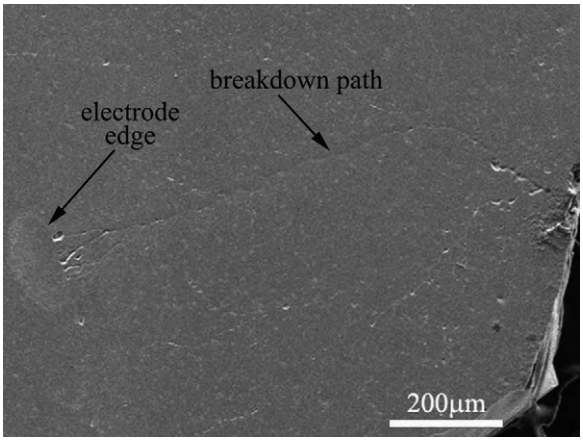

Fig. 8. Breakdown path on the sample surface.

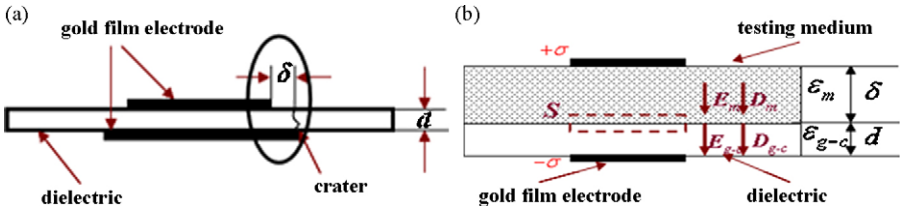

Fig. 9. Edge breakdown model: (a) schematic chart for the dielectric capacitor configuration and the crater location: d and δ are the thickness of the dielectric and the distance between the edge of the plane electrode and the crater, respectively; (b) the series model of the dielectric and the testing media in the breakdown position: ε_m and ε_{g-c} are the permittivity for testing media and dielectrics, respectively.

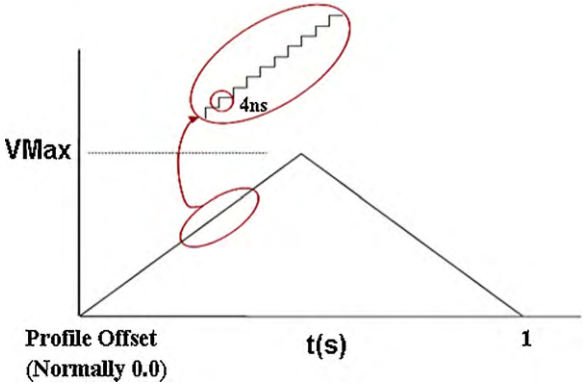

Fig. 10. Defining of the standard monopolar voltage profile on dielectrics.

Obviously, $E_m \approx 100E_{g-c}$ is estimated by $\varepsilon_{g-c} \approx 100\varepsilon_m$, where $\varepsilon_{g-c} = 100–500$, $\varepsilon_m = 1–5$. Therefore, the pre-failure of the low permittivity testing media leads to the low breakdown behavior of high dielectric constant glass-ceramics. The relation between the permittivity of the testing media and the dielectric strength is revealed in Fig. 7. It provides evidence that the dielectric strength of glass-ceramics tends to significantly increases with the increasing of the permittivity of testing liquid media.

4. Conclusion

By present work, it is shown that the testing media does have significant influences on the measured results in the determination process of dielectric properties for lead sodium niobate glass-ceramics. Five testing liquids with typical properties were considered. The results show that the measured leakage current of the dielectric depends on the conductivity of the testing media, while the resulted breakdown strength depends mostly on how high the dielectric constant of the media liquid is. The higher the electric conductivity of the testing media, the higher the obtained leakage current of the dielectric materials would be. The current–voltage (I–V) measurement taken in silicon/castor oil mixture (SCO) reveals the lowest leakage current density (LC = 6.72×10^{-6} A/cm^2, at $E = 25$ kV/mm) of the dielectric glass-ceramics. Compared to other liquid media, silicon/castor oil mixture leads to the thinnest polarization curve and comparatively low hysteresis value ($\Delta\varepsilon_r/\varepsilon_r$) as revealed by capacitance–voltage (C–V) measurement. Besides, it is shown that using dielectric liquids with higher dielectric constant as testing media would usually leads to a much higher breakdown strength, especially for dielectric materials with high ε_r and high EBD, as is the case for lead sodium niobate glass-ceramics. The measured breakdown strength of this material in glycerin (GE) can be as high as 105.6 kV/mm, which is about twice that measured in silicon oil (SO).

Acknowledgements

The authors acknowledge the financial support from the National High-tech Program (863 Program) under grant no. 2008AA03A236.

References

[1] M. Pollet, S. Marinel, G. Desgardin, $CaZrO_3$, a Ni-co-sinterable dielectric material for base metal-multilayer ceramic capacitor applications, J. Eur. Ceram. Soc. 24 (2004) 119–127.
[2] A.V. Polotai, T.H. Jeong, G.Y. Yang, et al., Effect of Cr additions on the microstructural stability of Ni electrodes in ultra-thin $BaTiO_3$ multilayer capacitors, J. Electroceram. 18 (2007) 261–268.
[3] J. Luo, J. Du, Q. Tang, C.H. Mao, Lead sodium niobate glass-ceramic dielectrics and internal electrode structure for high energy storage density capacitors, IEEE Trans. Electron. Dev. 55 (12) (2008) 3549–3554.
[4] Z.H. Wu, M.H. Cao, Z.Y. Shen, H.T. Yu, Z.H. Yao, D.B. Luo, H.X. Liu, Effect of glass additive on microstructure and dielectric properties of $SrTiO_3$ ceramics, Ferroelectrics 356 (2007) 95–101.
[5] Z.H. Wu, H.X. Liu, M.H. Cao, Z.H. Shen, Z.H. Yao, H. Hao, D.B. Luo, Effect of $BaO–Al_2O_3–B_2O_3–SiO_2$ glass additive on densification and dielectric properties of $Ba_{0.3}Sr_{0.7}TiO_3$ ceramics, J. Ceram. Soc. Jpn. 116 (2) (2008) 345–349.
[6] S.M. Lebedev, O.S. Gefle, Y.P. Pokholkov, V.I. Chichikin, The breakdown strength of two-layer dielectrics, in: High Voltage Engineering Symposium, 1999, 304–307.
[7] M.L. Krogh, B.C. Schultz, W. Huebner, et al., High breakdown strength, multilayer ceramics for compact pulsed power applications, in: IEEE Pulsed Power Conference, 1999, 1242–1245.
[8] J.J. Shyu, C.H. Chen, Sinterable ferroelectric glass-ceramics containing $(Sr,Ba)Nb_2O_6$ crystals, Ceram. Int. 29 (2003) 447–453.
[9] J. Liebault, J. Vallayer, D. Goeuriot, D. Treheux, F. Thevenot, How the trapping of charges can explain the dielectric breakdown performance of alumina ceramics, J. Eur. Ceram. Soc. 21 (2001) 389–397.
[10] J. Du, B. Jones, M. Lanagan, Preparation and characterization of dielectric glass-ceramics in $Na_2O–PbO–Nb_2O_5–SiO_2$ system, Mater. Lett. 59 (22) (2005) 2821–2826.
[11] S.M. Sze, Physics of Semiconductor Devices, J. Wiley & Sons, NY, 1981
[12] S.Y. Wang, B.L. Cheng, C. Wang, S.A.T. Redfern, S.Y. Dai, K.J. Jin, H.B. Lu, Y.L. Zhou, Z.H. Chen, G.Z. Yang, Influence of Ce doping on leakage current in $Ba_{0.5}Sr_{0.5}TiO_3$ films, J. Phys. D: Appl. Phys. 38 (2005) 2253–2257.
[13] A.I. Dedyk, E.A. Nenasheva, A.D. Kanareykin, Ju.V. Pavlova, O.V. Sinjukova, S.F. Karmanenko, Tunability and leakage currents of (Ba,Sr)-TiO_3 ferroelectric ceramics with various additives, J. Electroceram. 17 (2006) 433–437.

[14] M.A. Lampert, P. Mark, Current Injection in Solids, Academic Press, NY and London, 1970, p. 34.
[15] J.K. Kim, S.S. Kim, W.J. Kim, A.S. Bhalla, R. Guo, Enhanced ferroelectric properties of Cr-doped $BiFeO_3$ thin films grown by chemical solution deposition, Appl. Phys. Lett. 88 (2006) 132901.
[16] S. Sharma, D.A. Hall, Structural and ferroelectric characterization of BMZ–BF–PT ceramics, J. Electroceram. 20 (2008) 81–87.
[17] I.O. Owate, R. Freer, Dielectric breakdown of ceramics and glass ceramics, in: Proceedings of the Sixth International Dielectric Materials, Measurements and Applications Conference, 1992, pp. 443–446.